Received: 19 February 2019 | Revised: 6 May 2019 | Accepted: 7 May 2019

DOI: 10.1002/jrs.5637

RESEARCH ARTICLE

WILEY Journal of RAMAN SPECTROSCOPY

Temperature-induced phonon behavior in titanium disulfide (TiS_2) nanosheets

A. Dużyńska | J. Judek | K. Wilczyński | K. Zberecki | A. Łapińska | A. Wróblewska | M. Zdrojek

Faculty of Physics, Warsaw University of Technology, Warsaw, Poland

Correspondence
A. Dużyńska, Faculty of Physics, Warsaw University of Technology, Koszykowa 75, 00-662 Warsaw, Poland.
Email: anna.duzynska@pw.edu.pl

Funding information
National Science Centre, Grant/Award Number: 2015/19/N/ST5/02312; National Centre for Research and Development, Grant/Award Number: Techmatstrateg1/37012/3/NCBR/2017

Abstract

A detailed study of temperature-dependent phonon properties of exfoliated titanium disulphide (TiS_2) nanosheets probed by Raman spectroscopy in the 80- to 450-K temperature range is reported here. The TiS_2 Raman mode (E_g, A_{1g}, and Sh) positions exhibit linear shift dependences; however, in contradiction to typical behavior, the Sh mode surprisingly exhibits positive first-order temperature coefficient (χ=0.0592 cm^{-1}/K) with increase of the temperature. In addition, the widths of studied peaks typically increase with temperature and peak intensity ratio shows no changes proving that relative phonon population is not affected by temperature. Our findings can be useful for further analysis of phonon properties and determination of thermal conductivity of supported TiS_2 thin films for advanced electronics devices.

KEYWORDS

layered materials, TiS_2, titanium disulfide, thermal properties

Transition metal dichalcogenides (TMDCs) are layered materials, which have recently attracted considerable attention of the scientific community due to their exeptional opto-electronic, mechanical, and thermal properties.[1,2] The TMDCs exhibit a sandwich-like structure of transition metal (from groups 4–6) layer enclosed between two chalcogen layers (e.g. S, Se, or Te), characterized by in-plane covalent bonds and weaker out-of-plane bonds due to the van der Waals interactions. Interestingly, the properties of those materials might be controlled and tuned by the selection of transition metal and chalcogen atoms.[2,3]

Titanium disulfide (TiS_2) belongs to the TMDC family and is a semimetal with small indirect band gap that can be opened and tuned via oxidation,[4] stoichiometry modifications (e.g., $Ti_{1.023}S_2$), or defects.[5–7] The TiS_2 thin layers attract attention due to variety of possible applications, including thermoelectric devices,[8–10] biosensors,[11] energy storage,[12,13] solar cells[14,15] and may constitute a useful material for lithium-ion battery production.[16–18] In order to further explore the possibilities of TiS_2 applications in above-mentioned examples, one needs to fully understand the fundamental properties of this material, including phonon properties. Phonon properties can be investigated using Raman spectroscopy, which has been proved to be an excellent tool for characterization of structural, thermal, optical, and electronic properties of layered materials.[19–21] However, up to date, phonon properties (especially as a function of temperature) in titanium disulfide thin films are still poorly understood or unavailable. There are only few relatively old reports on Raman spectroscopy performed only for the bulk forms of TiS_2[22,23] or for Ag intercalated bulk material,[24] showing some temperature dependence of A_{1g} and E_g modes in the limited temperature range, however, without determination of first-order temperature coefficients. Additionally, only the comparison of the Raman spectra at 15 K and room temperature (RT) for the bulk TiS_2 was presented in Jiménez Sandoval et al.[24] Up to now, there are no reports showing the detailed temperature evolution of Raman modes for TiS_2 thin nanosheets.

Here, Raman spectroscopy was used to analyze the temperature-dependent phonon behavior of titanium disulfide thin films. We showed that the positions of the E_g and A_{1g} modes exhibit a typical decreasing linear temperature dependence directly resulting from the anharmonicity of the crystal lattice potential. However, the position of the A_{1g} broad shoulder mode (Sh) is linearly upshifted as a function of the temperature, which is an unexpected and intriguing behavior. Moreover, the first-order temperature coefficients (χ) for all observed Raman modes were extracted and compared with other 2D materials.

Fig.1a and 1b show crystal structure of analyzed 1*T*-phase of titanium disulfide from a side and top view, respectively. TiS_2 nanosheets were fabricated on SiO_2 (285nm)/Si substrate by conventional mechanical exfoliation technique[25,26] from a bulk single crystal (HQ Graphene). Atomic force microscopy image of investigated flake is presented in Fig. 1c, and the measured thickness is approximately 100 nm.

The Raman spectra were collected using a Renishaw inVia spectrometer in a backscattering configuration with a 514- and 633-nm laser excitation lines and a 50x objective. The diameter of the laser beam focused on the sample was approximately 1–2 μm, and the laser power (calibrated on the sample) equals 2 mW. Parameters of the laser beam were carefully selected to obtain the maximal signal to noise ratio without sample heating. We verified that a change in laser power up to 2 mW (at RT) does not affect the Raman peak position in supported TiS_2 layer. Fig. 1d shows typical Raman spectrum of the analyzed sample, taken at RT. The Lorentzian functions were fitted to the experimental data to designate the positions, full widths at half maximum (FWHM), and intensities of Raman modes (see the Supporting Information for details of error estimation).

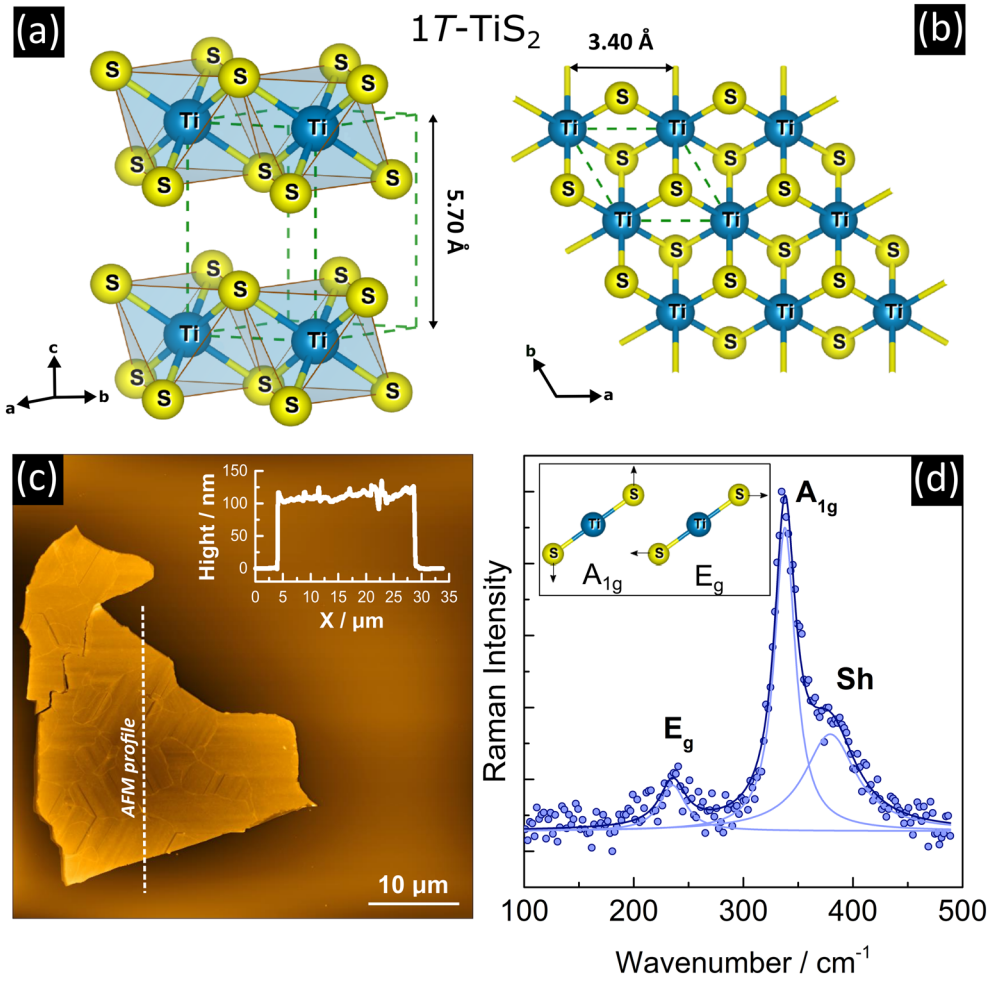

FIGURE 1 Crystal structure of titanium disulfide: (a) a side view and (b) a top view; the lattice constants (in Å units) were marked. Atomic force microscopy (AFM) image of TiS_2 flake (c); inset shows the corresponding AFM height profile. Typical Raman spectrum of TiS_2 flake obtained with $\lambda_{ex} = 514$ nm at room temperature (d); inset shows vibrations of Raman active modes for 1*T*-phase titanium disulfide [Colour figure can be viewed at wileyonlinelibrary.com]

The temperature-dependent Raman measurements were performed with a Linkam DSC600 optical cell system (0.1-K resolution) in the range of 80–450 K, at nitrogen atmosphere. We emphasize that studied samples were put into the cryostat immediately after exfoliation in air, in order to minimize the oxidation effects. For each temperature, the spectra were collected several times in order to reduce the statistical error. Moreover, the Raman measurements as a function of the temperature were repeated on a few samples with different thicknesses to confirm the trends in results. The comparison of Raman spectra for different thicknesses of TiS_2 flakes (in the range 50–200 nm) acquired using 514-nm excitation laser line (and additionally with 633 nm) is included in Fig. S1 in the Supporting Information. For both excitations lines there were no observable changes in positions and FWHM of Raman modes as a function of the flake thickness (see Fig. S2 and S3). Similarly, the flake thickness dependence of the Raman modes' intensity ratio shows slight changes (see Fig. S4). We note that the Raman spectra of TiS_2 flakes thinner than 65 nm have very low signal to noise ratio, what is probably related with sulfur vacancies and/or intercalated Ti ions, other defects in the titanium disulfide thin film structures,[27–29] or more likely low absorption coefficient of TiS_2, or faster structural degradation of very thin TiS_2 layers as observed for others 2D materials.[30]

Titanium disulfide is a 4-6 layered material, and it crystallizes (at RT) into trigonal structure with a space group $P\bar{3}m1$. For 1*T* TiS_2, there are three atoms per unit cell (the crystal symmetry is described by the $D_{\bar{3}}d^3$ point group[31]) and the decomposition into irreducible representations at Γ point is given by $\Gamma = A_{1g}+E_g+2A_{2u}+2E_u$, where modes with A_{1g} and E_g symmetry are the Raman active modes and modes with $2A_{2u}$ and $2E_u$ symmetry are the infrared active modes.[32] The E_g (~234 cm^{-1} at RT) and A_{1g} (~336 cm^{-1} at RT) modes correspond to the in-plane and out-of-plane vibrations of sulfur atoms, respectively[33] (see inset in Fig. 1d). Additionally, in the TiS_2 Raman spectra a "broad shoulder" appears at ~369 cm^{-1} at RT on the high-energy side of the A_{1g} peak, and for the sake of clarity, in this work called Sh (see Fig. 1d). This feature is also observed for bulk TiS_2.[22,23] The possible origin of this peak is still under discussion. Sandoval et al. suggested that this feature can originate from overtone and/or summation processes.[24] However, other study correlates this mode with defects in TiS_2 structure resulting from the excess interlayer titanium atoms, which cause local stiffening of the phonons and involve motion of the sulfur atoms transverse to the layer.[34] The latter hypothesis has been repeated by other work on chemically exfoliated TiS_2 nanosheets by a lithium borohydride intercalation.[29] Authors of this work showed that the A_{1g} shoulder appears more pronounced for multilayers than monolayers and thus can be useful for the determination of the layers numbers (up to six layers). Other possible explanation of this peak's origin, including stress, A_{2u} peak appearance, and double resonant effect is discussed in Ranalli.[35]

Fig. 2a presents a set of Raman spectra of approximately 100-nm-thick TiS_2 flake for selected temperatures between 80 and 450 K. As the temperature increases, the E_g and A_{1g} Raman modes soften linearly and clearly broaden. Fig. 2b and 2c show the detailed temperature dependence of the Lorentzian-fit peak positions for the E_g and A_{1g} phonons. The evolution of the E_g and A_{1g} phonon wavenumbers ω (in cm^{-1} units) as a function of the temperature shows a linear behavior according to relation

$$\omega(T) = \omega_0 + \chi T, \quad (1)$$

where ω_0 is the phonon wavenumber for temperature extrapolated to 0 K, χ is the first-order temperature coefficient, and T is the absolute temperature.[36–39] The linear dependence of phonon wavenumbers in TiS_2 thin layers are related to the anharmonicity of the interatomic potential,[36,40] which results in phonon energy renormalization and thermal expansion, which can also modify the force constants. The calculated fitting parameters from Equation (1) are shown in Table 1. The extracted linear temperature coefficients (χ) from the slopes equal –0.0386 $cm^{-1}/K \pm 0.0021$ cm^{-1}/K and –0.0134 $cm^{-1}/K \pm 0.0005$ cm^{-1}/K for the E_g and A_{1g} Raman modes, respectively. We notice that the χ value for E_g mode is clearly higher compared with A_{1g} mode, which indicates more significant temperature impact on phonon vibrations across *b*-axis than to *c*-axis (possibly due to the different nature of the intraplane covalent bonding or/and the interlayer van der Waals bonding or/and different symmetry of those phonons) and can affect the anisotropic thermal expansion of the 1T-TiS_2 crystal.[36,41] Interestingly, the calculated values of χ parameter for the E_g and A_{1g} titanium disulfide Raman modes are comparable with those reported for other 2D materials (TiS_3,[42] black phosphorus,[38] WS_2,[43] MoS_2,[44] or graphene[36]), which are summarized in Table 1.

An interesting feature is seen for the temperature dependence of Sh peak position shown in Fig. 2d. Namely, the broad shoulder of A_{1g} peak is linearly upshifted from 358.9 to 378.8 cm^{-1} in range of 80–450 K, giving the slope of the fitted line dependence that equals $+0.0592$ $cm^{-1}/K \pm 0.0063$ cm^{-1}/K. The first striking property is the positive peak position shift with temperature, and the second is that magnitude of the shift for the given temperature range equals almost 20 cm^{-1}, showing very strong temperature impact. We note that a small positive

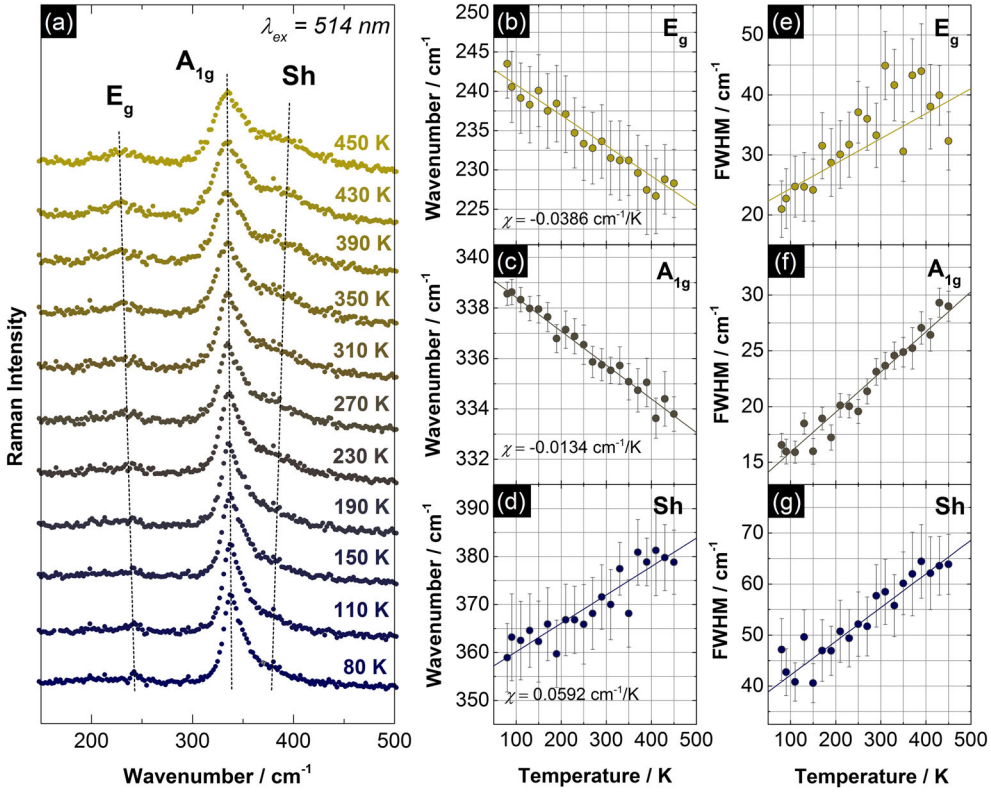

FIGURE 2 Selected Raman spectra of TiS_2 measured in 80- to 450-K temperature range (a). Temperature dependence of (b-d) positions and (e-g) full widths at half maximum (FWHMs) of E_g, A_{1g}, and Sh Raman modes in TiS_2 [Colour figure can be viewed at wileyonlinelibrary.com]

value of χ coefficient was also reported for the phonon with E (TO) symmetry in α-quartz (0.010 $cm^{-1}/K \pm 0.005$ cm^{-1}/K) and hexagonal GeO_2 (0.005 $cm^{-1}/K \pm 0.002$ cm^{-1}/K) and for the B_{1g} mode in tetragonal GeO_2 (0.003 $cm^{-1}/K \pm 0.001$ cm^{-1}/K).[41] We also note that the impact of the substrate thermal expansion should be negligible due to the TiS_2 flake thickness (~100 nm). It seems that the origin of the Sh needs to be verified with theoretical calculation of phonon structure of TiS_2 with including impact of the interlayer defects.

Fig. 2e-g present widths of E_g, A_{1g}, and Sh modes (that are usually inversely proportional to the phonon lifetime), respectively, in the 80- to 450-K temperature range. The linewidth of all peaks clearly broadens with the temperature increase and indicates approximately rather typical linear relation (similar trend has been observed for

TABLE 1 Calculated parameters from fit of Equations (1) and (2) to temperature dependence of the positions and FWHMs of TiS_2 Raman modes compared with literature data for selected 2-D materials

Raman mode/material type	ω_0 (cm^{-1}) Equation (1)	χ (cm^{-1}/K) Equation (1)	Γ_0 (cm^{-1}) Equation (2)	C (cm^{-1}/K) Equation (2)	Ref.
E_g/TiS_2 flakes	244.7	-0.0386	20.2	0.042	This work
A_{1g}/TiS_2 flakes	339.7	-0.0134	12.3	0.036	This work
Sh/TiS_2 flakes	354.2	+0.0592	35.6	0.066	This work
A_{1g}/TiS_3 nanosheets	-	from -0.0170 to -0.0283	-	-	Pawbake et al.42
A_g^2/black phosphorus few-layer	-	-0.0283	-	-	Łapińska et al. 38
A_{1g}/WS_2 monolayer	-	-0.0121	-	-	Huang et al. 43
E_{2g}^1/WS_2 monolayer	-	-0.0091	-	-	Huang et al. 43
A_{1g}/MoS_2 few-layer	408.4	-0.0123	-	-	Sahoo et al. 44
E_{2g}^1/MoS_2 few-layer	382.6	-0.0132	-	-	Sahoo et al. 44

Abbreviation: FWHMs: full widths at half maximum.

other 2D materials, e.g., graphene and h-BN[45]). In order to quantitatively describe the evolution of FWHMs as a function of the temperature, the Equation (2) is applied[45]

$$\Gamma(T) = \Gamma_0 + CT, \quad (2)$$

where Γ_0 is the FWHM at 0 K and C stands for fitting constant. The calculated Γ_0 and C values are shown in Table 1. The relative change of the peaks width, in temperature range of 80–450 K, equals 11.4, 12.5, and 16.7 cm^{-1} for the E_{1g}, A_{1g}, and Sh peaks, respectively. This suggests that the Sh mode width is slightly more sensitive to temperature variation as compared with E_g and A_{1g} modes. Interestingly, in the contrary to the peak position, the Sh mode exhibits typical temperature dependency of the peak width (increase with temperature). Only, for the E_g mode (Fig. 2e), the Raman spectrum has a relatively low signal intensity and the width determination has relatively large error. According to thermal transport models, the lattice thermal conductivity is directly proportional to the phonon lifetime.[46] Thus, broadening of the peak widths may suggest the decrease of thermal conductivity (and thermal diffusivity) of the TiS_2 with temperature. However, this effect remains to be studied.

Fig. S5 shows the temperature dependence of the relative intensity ratio of the A_{1g} and Sh modes. Clearly, there is no significant change in $I(A_{1g})/I$ (Sh) coefficient within the investigated temperature range. Constant value of above coefficient indicates that temperature variation has no influence on the relative population of A_{1g} and Sh phonons. Because of the fact that Sh phonon nature is still not fully understood, the explanation of this observation needs further theoretical studies.

1 | CONCLUSIONS

In conclusion, we have performed the temperature-dependent Raman studies of mechanically exfoliated titanium disulfide thin films supported on SiO_2/Si substrate and determined their phonon properties in temperature range between 80 and 450 K. The first order temperature coefficients were calculated and are χ = -0.0283, -0.0134, and +0.0592 cm^{-1}/K for E_g, A_{1g}, and Sh modes, respectively. These results can be also useful for further analysis of phonon properties and deeper understanding of heat dissipation of supported TiS_2 films, using, for example, optothermal method.[47]

ACKNOWLEDGEMENTS

This work has been partially supported by the National Centre for Research and Development under grant Techmatstrateg1/37012/3/NCBR/2017. A. Ł. acknowledges support from the project Preludium funded by the National Science Centre (2015/19/N/ST5/02312).

ORCID

A. Dużyńska https://orcid.org/0000-0001-8006-3914
J. Judek https://orcid.org/0000-0002-4326-7392
A. Łapińska https://orcid.org/0000-0002-7005-9273
A. Wróblewska https://orcid.org/0000-0003-3728-1216
M. Zdrojek https://orcid.org/0000-0002-8897-6205

REFERENCES

[1] Z. Lin, A. McCreary, N. Briggs, S. Subramanian, K. Zhang, Y. Sun, X. Li, N. J. Borys, H. Yuan, S. K. Fullerton-Shirey, A. Chernikov, H. Zhao, S. McDonnell, A. M. Lindenberg, K. Xiao, B. J. LeRoy, M. Drndić, J. C. M. Hwang, J. Park, M. Chhowalla, R. E. Schaak, A. Javey, M. C. Hersam, J. Robinson, M. Terrones, *2D Mater.* **2016**, *3*, 042001.

[2] G. R. Bhimanapati, Z. Lin, V. Meunier, Y. Jung, J. Cha, S. Das, D. Xiao, Y. Son, M. S. Strano, V. R. Cooper, L. Liang, S. G. Louise, E. Ringe, W. Zhou, S. S. Kim, R. R. Naik, B. G. Sumpter, H. Terrones, F. Xia, Y. Wang, J. Zhu, D. Akinwande, N. Alem, J. A. Schuller, R. E. Schaak, M. Terrones, J. A. Robinson, *ACS Nano* **2015**, *9*, 11509.

[3] Q. H. Wang, K. Kalantar-Zadeh, A. Kis, J. N. Coleman, M. S. Strano, *Nat. Nanotechnol.* **2012**, *7*, 699.

[4] T. Umebayashi, T. Yamaki, H. Itoh, K. Asai, *Appl. Phys. Lett.* **2002**, *81*, 454.

[5] J. A. Wilson, *Solid State Commun.* **1977**, *22*, 551.

[6] C. Riekel, R. Schöllhorn, *Mater. Res. Bull.* **1975**, *10*, 629.

[7] J. Bernard, Y. Jeannin, in *Symposium of Nonstoichiometric Compounds*, (Ed: R. Ward) *Adv. in Chem. Ser.* 39, American Chemical Society, New York **1963** 191.

[8] R. Tian, C. Wan, Y. Wang, Q. Wei, T. Ishida, A. Yamamoto, A. Tsuruta, W. Shin, S. Li, K. Koumoto, *J. Mater. Chem. A* **2017**, *5*, 564.

[9] Y. Zhou, J. Wan, Q. Li, L. Chen, J. Zhou, H. Wang, D. He, X. Li, Y. Yang, H. Huang, *ACS Appl. Mater. Interfaces* **2017**, *9*, 42430.

[10] C. Wan, X. Gu, F. Dang, T. Itoh, Y. Wang, H. Sasaki, M. Kondo, K. Koga, K. Yabuki, G. J. Snyder, R. Yang, K. Koumoto, *Nat. Mater.* **2015**, *14*, 622.

[11] Z. Li, X. Ding, Y. Li, L. Wang, J. Fan, *Nanoscale* **2016**, *8*, 9852.

[12] C. G. Hawkins, L. Whittaker-Brooks, *ACS Appl. Nano Mater.* **2018**, *1*, 851.

[13] C. Wan, R. Tian, A. B. Azizi, Y. Huang, Q. Wei, R. Sasai, S. Wasusate, T. Ishida, K. Koumoto, *Nano Energy* **2016**, *30*, 840.

[14] X. Meng, C. Yu, B. Lu, J. Yang, J. Qiu, *Nano Energy* **2016**, *22*, 59.

[15] G. Yin, H. Zhao, J. Feng, J. Sun, J. Yan, Z. Liu, S. Lin, S. F. Liu, *J. Mater. Chem. A* **2018**, *6*, 9132.

[16] D. Y. Oh, Y. E. Choi, D. H. Kim, Y.-G. Lee, B.-S. Kim, J. Park, H. Sohn, Y. S. Jung, *J. Mater. Chem. A* **2016**, *4*, 10329.

[17] W. Sun, L. Suo, F. Wang, N. Eidson, C. Yang, F. Han, Z. Ma, T. Gao, M. Zhu, C. Wang, *Electrochem. Commun.* **2017**, *82*, 71.

[18] B. Kartick, S. K. Strivastava, S. Mahanty, *J. Nanopart. Res.* **2013**, *15*, 1950.

[19] X. Zhang, X.-F. Qiao, W. Shi, J.-B. Wu, D.-S. Jiang, P.-H. Tan, *Chem. Soc. Rev.* **2015**, *44*, 2757.

[20] A. Nikolenko, V. Strelchuk, O. Gnatyuk, P. Kraszkiewicz, V. Boiko, E. Kovalska, W. Mista, R. Klimkiewicz, V. Karbivskii, G. Dovbeshko, *J. Raman Spectrosc.* **2019**, *50*, 490.

[21] G. Amato, F. Beccaria, E. Landini, E. Vittone, *J. Raman Spectrosc.* **2019**, *50*, 499.

[22] R. Leonelli, Raman Scattering in Silver Intercalated Titanium Disulphide, *A Thesis of Master of Science*, Simon Fraser University, **1980**.

[23] M. Hangyo, S. Nakashima, Y. Hamada, T. Nishio, Y. Ohno, *Phys. Rev. B* **1993**, *48*, 11291.

[24] S. Jiménez Sandoval, X. K. Chen, J. C. Irwin, *Phys. Rev. B* **1992**, *45*, 14347.

[25] K. S. Novoselov, D. Jiang, F. Schedin, T. J. Booth, V. V. Khotkevich, S. V. Morozov, A. K. Geim, *Proc. Natl. Acad. Sci. U. S. A.* **2005**, *102*, 10451.

[26] K. S. Novoselov, A. K. Geim, S. V. Morozov, D. Jiang, Y. Zhang, S. V. Dubonos, I. V. Grigorieva, A. A. Frisov, *Science* **2004**, *306*, 666.

[27] D. Ma, Q. Wang, T. Li, C. He, B. Ma, Y. Tang, Z. Lu, Z. Yang, *J. Mater. Chem. C* **2016**, *4*, 7093.

[28] Z. Lin, B. R. Carvalho, E. Khan, R. Lv, R. Rao, H. Terrones, M. A. Pimenta, and M. Terrones, *2D Mater.* 2016; *3*, 022002.

[29] P. C. Sherrell, K. Sharda, C. Grotta, J. Ranalli, M. S. Sokolikova, F. M. Pesci, P. Palczynski, V. L. Bemmer, C. Mattevi, *ACS Omega* **2018**, *3*, 8655.

[30] R. Frisenda, E. Navarro-Moratalla, P. Gant, D. Pérez De Lara, P. Jarillo-Herrero, R. V. Gorbachev, A. Castellanos-Gomez, *Chem. Soc. Rev.* **2018**, *47*, 53.

[31] M. Plischke, K. K. Bardhan, R. Leonelli, J. C. Irwin, *Can. J. Phys.* **1983**, *61*, 397.

[32] G. Lucovsky, W. Y. Liang, R. M. White, K. R. Pisharody, *Solid State Commun.* **1976**, *19*, 303.

[33] M. Ishii, M. Saeki, I. Kawada, *Phys. Status Solidi B* **1984**, *124*, K109.

[34] P. C. Klipstein, A. G. Bagnall, W. Y. Liang, E. A. Marseglia, R. H. Friend, *J. Phys. C: Solid State Phys.* **1981**, *14*, 4067.

[35] J. Ranalli, Dimensionality Effect of Titanium Disulphide Nanosheets on its Vibrational Properties Measured via Raman Spectroscopy, *A Thesis of Master of Science*, Politecnico Di Milano, **2016**.

[36] I. Calizo, S. Ghosh, W. Bao, F. Miao, C. N. Lau, A. A. Balandin, *Solid State Commun.* **2009**, *149*, 1132.

[37] A. Taube, A. Łapińska, J. Judek, M. Zdrojek, *Appl. Phys. Lett.* **2015**, *107*, 013105.

[38] A. Łapińska, A. Taube, J. Judek, M. Zdrojek, *J. Phys. Chem. C* **2016**, *120*, 5265.

[39] A. Taube, A. Łapińska, J. Judek, N. Wochtman, M. Zdrojek, *J. Phys. D: Appl. Phys.* **2016**, *49*, 315301.

[40] R. Yan, J. R. Simpson, S. Bertolazzi, J. Brivio, M. Watson, X. Wu, A. Kis, T. Luo, A. R. Hight Walker, H. G. Xing, *ACS Nano* **2014**, *8*, 986.

[41] P. Gillet, A. Le Cléac'h, M. Madon, *J. Geophys. Res.* **1990**, *95*, 21635.

[42] A. S. Pawbake, J. O. Island, E. Flores, J. R. Ares, C. Sanchez, S. J. Ferrer, S. R. Jadkar, H. S. J. van der Zant, A. Castellanos-Gomez, D. J. Late, *ACS Appl. Mater. Interfaces* **2015**, *7*, 24185.

[43] X. Huang, Y. Gao, T. Yang, W. Ren, H.-M. Cheng, T. Lai, *Sci. Rep.* **2016**, *6*, 32236.

[44] S. Sahoo, A. P. S. Gaur, M. Ahmadi, M. J.-F. Guniel, R. S. Katiyar, *J. Phys. Chem. C* **2013**, *117*, 9042.

[45] X. Li, J. Liu, K. Ding, X. Zhao, S. Li, W. Zhou, B. Liang, *Nanoscale Res. Lett.* **2018**, *13*, 25.

[46] P. G. Klemens, in *Solid State Physics*, (Eds: F. Seitz, D. Turnbull), Academic Press, New York **1958**.

[47] J. Judek, A. P. Gertych, M. Świniarski, A. Łapińska, A. Dużyńska, M. Zdrojek, *Sci. Rep.* **2015**, *5*, 12422.

SUPPORTING INFORMATION

Additional supporting information may be found online in the Supporting Information section at the end of the article.

How to cite this article: Dużyńska A, Judek J, Wilczyński K, et al. Temperature-induced phonon behavior in titanium disulfide (TiS_2) nanosheets. *J Raman Spectrosc*. 2019;50:1114–1119. https://doi.org/10.1002/jrs.5637